Journal of Solid Mechanics Vol. 10, No. 1 (2018) pp. 38-56

Non Uniform Rational B Spline (NURBS) Based Non-Linear Analysis of Straight Beams with Mixed Formulations

R. Ranjan [1, *], J.N. Reddy [2]

[1] *School of Aerospace and Mechanical Engineering, 865 Asp Avenue, Norman, OK, 73019, USA*
[2] *Department of Mechanical Engineering, 3123 TAMU, College Station, TX, USA*

Received 3 September 2017; accepted 6 December 2017

ABSTRACT

Displacement finite element models of various beam theories have been developed traditionally using conventional finite element basis functions (i.e., cubic Hermite, equi-spaced Lagrange interpolation functions, or spectral/hp Legendre functions). Various finite element models of beams differ from each other in the choice of the interpolation functions used for the transverse deflection w, total rotation φ_x , and/or shear strain Υ_{xz} , as well as the variational method used (e.g., collocation, weak form Galerkin, or least-squares). When nonlinear shear deformation theories are used, the displacement finite element models experience membrane and shear locking. The present study is concerned with development of alternative beam finite elements using both uniform and non-uniform rational b-splines (NURBS) to eliminate shear and membrane locking in an hpk finite element setting for both the Euler-Bernoulli beam and Timoshenko beam theories. Both linear and non-linear analysis are performed using mixed finite element models of the beam theories studied. Results obtained are compared with analytical (series) solutions and non-linear finite element and spectral/hp solutions available in the literature, and excellent agreement is found for all cases.

Keywords: NURBS basis; Euler-Bernoulli beam theory; Timoshenko beam theory; B-splines; Mixed formulation.

1 INTRODUCTION

THREE different kinematic theories have been used to study beams, namely, Euler-Bernoulli theory (EBT), Timoshenko beam theory (TBT), and Reddy third-order shear deformation theory (RBT) [1]. The displacement finite element models of TBT and RBT are known to exhibit shear locking when using equal-order, lower-order interpolation of the generalized displacements (w, φ_x). Locking is due to inconsistency of the interpolation used for w and φ_x . Often reduced-order integration techniques are used to alleviate locking [2]. The reduced integration beam elements are known to exhibit spurious energy modes. Others have used so-called consistent interpolations based on the recovery of correct constraints in the thick beam limit [3, 4]. Although such elements do not experience locking, they did not lead to the two-node super-convergent element developed by Reddy [5], who used the cubic Hermite interpolation of w and interdependent quadratic interpolation of φ_x in developing the element. The

*Corresponding author.
E-mail address: ranrakesh@gmail.com (R.Ranjan).

conventional reduced integration Timoshenko elements as well as consistent interpolated quadratic elements fail to capture the true behavior of such members unless two or more elements per structural member are used. While the displacement-based models for the Timoshenko beam theory (TBT) admit the use of C^0 expansions, the use of the Euler Bernoulli beam theory (EBT) requires the use of C^1-continuous expansion of w and C^0-interpolation of φ_x. The mixed formulation in which stress resultants are incorporated into the fundamental governing equations for the Euler Bernoulli beam theory admits the use of C^0 expansions [6]. The use of b-spline basis offers higher continuity and C^1 continuous hierarchal expansions lends itself to spectral accuracy. The TBT on the other hand, allows the use of C^0 approximations for the displacement based formulations. In the thin beam limit, the TBT model should provide similar results as the EBT. However due to the use of equal lower-order (i.e., linear) approximations for the displacements and rotation, the element fails to realize the thin beam limit and thus experiences shear locking. Most studies in literature make use of equi-spaced Lagrange higher-order expansions for studying the bending response (see Arciniega and Reddy [7]). The equi-spaced Lagrange approximation functions suffer from severe ill-conditioning for high values of the polynomial degree p [8]. At high p_{levels} the discrete problem suffers from a very high condition number of the stiffness matrix and the problem exhibits poor convergence behavior. The choice of higher-order approximation functions has a dramatic effect on the conditioning of the discrete problem. Significant amount of work has been done to improve higher-order finite elements or p-version FEM [9-13]. Low order finite element methods for solving beam problems exhibit either membrane or shear locking. This problem is commonly treated by reduced integration techniques, although other remedies may be found [2, 13]. Shear locking is evident in the weak-form displacement finite element models of TBT with equal-order interpolation of the generalized displacements. The phenomenon is more predominant when the length-to-thickness ratio of the beam is large. Higher-order elements have been explored in literature to alleviate shear locking but they have been mostly based on equi-spaced Lagrange polynomials. The use of spectral/hp nodal expansions was first explored by Ranjan [13], who used nodal expansions to study the bending response of EBT, TBT, and plates with both displacement based and mixed formulations. There has been increased interest in the past decade on using b-spline based iso-geometric method for studying vibration response [14] and bending response of third order shear deformation theory [15]. Non-linear analysis of the Euler-Bernoulli beam theory and the Timoshenko beam theory was performed with spectral/hp methods by Ranjan and Reddy [12, 16].

Isogeometric methods (IGA) have been proposed as a new computational paradigm for solving partial differential equations which enable an elegant integration of the computer aided design (CAD) in an hpk framework [17]. Isogeometric collocation methods were used to solve the Timoshenko beam theory by [14]. An isogeometric collocation approach for solving the Euler Bernoulli beam theory was demonstrated by [18]. An isogeometric analysis (IGA) for solving the static EBT beam deflection and vibrations were performed in [19]. Third-order shear deformation theory (TSDT) was analyzed with an iso-geometric approach in [20] and for laminated composite plates for first order shear deformation theory FSDT) in Kapoor and Kapania [21]. Thus both isogeometric collocation approach and weak form Galerkin finite element methods have been examined for solving displacement based formulations for EBT, TBT, and third-order shear deformation theory of Reddy (RBT) [22]. However, literature is lacking in examining mixed formulations for solving deflection of both EBT and TBT, especially using NURBS. We utilize non uniform b-spline basis (NURBS) functions within the framework of mixed formulations to develop beam finite elements. The motivation for this study comes from the many advantages associated with b-spline basis functions; spectral convergence (accuracy) of the solution, avoidance of locking (with displacement based formulations), mixed formulations lend themselves to locking avoidance naturally, control of continuity across the knot index space, and partition of unity. Different length-to-thickness, *a/h*, ratios are examined and with appropriate hpk-refinements full integration was found to provide consistently good agreement with published results for both linear and non-linear problems.

2 BEAM THEORIES MIXED FORMULATIONS

The EBT is based on the assumption that a straight line transverse to the axis of the beam remains straight, inextensible, and normal to the mid-plane after deformation. These assumptions amount to neglecting the Poisson effect and the transverse normal and shear strains. The displacement field for beams with moderately large rotations but with small strains (i.e., the von Karman non-linearity) can be derived using the displacement field (EBT)

$$u_1(x,z)=u(x)-z\frac{\partial w}{\partial x} \quad , \quad u_2(x,z)=0 \quad , \quad u_3(x,z)=w(x) \tag{1}$$

where (u_1,u_2,u_3) denote the total displacements along the three coordinate directions (*x, y, z*), and *u* and *w* denote the axial and transverse displacements of a point on the neutral axis. The only nonzero von Karman non-linear strain is given by

$$\varepsilon_{xx}=\frac{\partial u}{\partial x}+\frac{1}{2}\left(\frac{\partial u}{\partial x}\right)^2-z\frac{\partial^2 w}{\partial x^2} \tag{2}$$

The Euler-Lagrange equations for the EBT can be derived using the principle of virtual work. For details on the virtual work principle the reader is referred to Reddy [2, 6]. Based on the virtual work principle and separating the virtual displacements we obtain the Euler Lagrange equations for the EBT as follows:

$$\frac{\partial N_{xx}}{\partial x}+f_x=0 \tag{3}$$

$$\frac{\partial V_x}{\partial x}+q_x=0 \tag{4}$$

$$V_x-\frac{\partial M_{xx}}{\partial x}-N_{xx}\frac{\partial w_0}{\partial x}=0 \tag{5}$$

where f_x is the distributed axial load and q_x is the distributed transverse load. In the EBT, Eq. (4) is used in Eq. (5) to replace V_x, and the resulting two equations govern the equilibrium of forces.

Assuming a linearly elastic behavior of the material, the relationship between the stress resultants (N_{xx},M_{xx}) and the generalized displacements (u,w,φ_x) can be expressed as:

$$N_{xx}=EA\left[\frac{\partial u_0}{\partial x}+\frac{1}{2}\left(\frac{\partial w_0}{\partial x}\right)^2\right] \tag{6}$$

$$M_{xx}=EI\frac{\partial \varphi_x}{\partial x}=-EI\frac{\partial^2 w_x}{\partial x^2} \tag{7}$$

$$\theta_x+\frac{\partial w_0}{\partial x}=0 \tag{8}$$

Timoshenko beam theory relaxes the normality restriction of the Euler-Bernoulli beam theory and allows for arbitrary but constant rotation of the transverse normals. The displacement field of the Timoshenko beam theory is:

$$u_1(x,z)=u_0(x)+z\varphi_x \quad , \quad u_2(x,z)=0 \quad , \quad u_3(x,z)=w_0(x) \tag{9}$$

The equilibrium equations of the TBT theory are provided as:

$$\frac{\partial N_{xx}}{\partial x}+f_x=0 \tag{10}$$

$$\frac{\partial M_{xx}}{\partial x}-Q_x=0 \tag{11}$$

$$\frac{\partial Q_{xx}}{\partial x}+\frac{\partial}{\partial x}\left(N_{xx}\frac{\partial w_0}{\partial x}\right)+q=0 \tag{12}$$

where φ_x is the rotation of a transverse normal about the y axis. The equations of equilibrium of the Timoshenko beam theory are the same as in Eqs. (10)- (12), with the stress resultants (N_{xx}, M_{xx}, Q_x) are given in terms of (u, w, φ_x) as:

$$N_{xx}=EA\left[\frac{\partial u_0}{\partial x}+\frac{1}{2}\left(\frac{\partial w_0}{\partial x}\right)^2\right] \tag{13}$$

$$M_{xx}=EI\frac{\partial \varphi_x}{\partial x} \tag{14}$$

$$Q_x=S_{xx}\left[\frac{\partial w_0}{\partial x}+\varphi_x\right] \tag{15}$$

The axial force N_{xx}, the bending moment M_{xx}, and the transverse shear force Q_x are defined by

$$N=\int_A \boldsymbol{\sigma}_{xx}dA \;,\; M=D_{xx}\frac{d\varphi_x}{dx} \;,\; Q_x=K_s\int_A \sigma_{xx}dA=S_{xx}\left(\frac{\partial w_0}{\partial x}+\varphi_x\right) \tag{16}$$

where K_s is the shear correction coefficient. The non-linearity in both theories comes from the von Karman non-linear strain. For a complete treatment of the EBT and TBT with the displacement based formulations and the derivation of the weak forms, the reader is referred to Reddy [2]. For the descriptions of beam theories with different mixed formulations the reader is referred to Ranjan [12, 13].

3 FINITE ELEMENT FORMULATION (EBT)

The governing equations of the Euler-Bernoulli beam theory can be expressed in several forms using different variables [13], and different finite element models can be developed. In this section we examine the mixed finite element formulation for beams. The governing equations for an EBT beam undergoing static deformations is:

$$\begin{aligned}
&\frac{\partial N_{xx}}{\partial x}+f_x=0 \quad,\quad \frac{\partial V_x}{\partial x}+q_x=0 \quad,\quad V_x-\frac{\partial M_{xx}}{\partial x}-N_{xx}\frac{\partial w_0}{\partial x}=0\\
&N_{xx}=EA\left[\frac{\partial u_0}{\partial x}+\frac{1}{2}\left(\frac{\partial w_0}{\partial x}\right)^2\right] \quad,\quad M_{xx}=EI\frac{\partial \varphi_x}{\partial x}=-EI\frac{\partial^2 w_x}{\partial x^2} \quad,\\
&\theta_x+\frac{\partial w_0}{\partial x}=0
\end{aligned} \tag{17}$$

The development of the weak finite element models for the equations follows multiplication of the above with a weight function and integration by parts. Assigning the variables in the formulation in the order: ($u, w, \theta_x, N_{xx}, V_x, M_x$). For the mixed model considered for analysis, the equations are kept in their primitive forms and the resulting formulation has six degrees of freedom per node. The finite element formulation follows standard procedures as detailed earlier. The nonzero terms of the stiffness matrix are obtained as follows:

$$K^{14}_{ij}=\int_{x_a}^{x_b}\frac{\partial\psi_i}{\partial x}\psi_j dx \;,\; F^1=\int_{x_a}^{x_b}\psi_i f_x dx \;,\; K^{25}_{ij}=\int_{x_a}^{x_b}\left[\frac{\partial\psi_i}{\partial x}\psi_j\right]dx \;,\; F^2=\int_{x_a}^{x_b}\psi_i q_x dx \;,$$
$$K^{35}_{ij}=\int_{x_a}^{x_b}\psi_i\psi_j dx \;,\; K^{36}_{ij}=\int_{x_a}^{x_b}\frac{\partial\psi_i}{\partial x}\psi_j dx \;,\; K^{34}_{ij}=\int_{x_a}^{x_b}\theta^x\psi_i\psi_j dx \;,\; F^3=0 \;,$$
$$K^{41}_{ij}=\int_{x_a}^{x_b}EA\left[\psi_i\frac{\partial\psi_j}{\partial x}\right]dx \;,\; K^{43}_{ij}=\int_{x_a}^{x_b}\frac{1}{2}EA\psi_i\psi_j\left(\frac{\partial\omega_o}{\partial x}\right)dx \;,\; K^{44}_{ij}=-\int_{x_a}^{x_b}\psi_i\psi_j dx \;,\; F^4=0 \;, \tag{18}$$
$$K^{52}_{ij}=\int_{x_a}^{x_b}\left(\psi_i\frac{\partial\psi_j}{\partial x}\right)dx \;,\; K^{53}_{ij}=\int_{x_a}^{x_b}\left[\psi_i\psi_j\right]dx \;,\; F^5=0 \;,\; K^{63}_{ij}=\int_{x_a}^{x_b}EI\left[\psi_i\frac{\partial\psi_j}{\partial x}\right]dx \;,$$
$$K^{66}_{ij}=\int_{x_a}^{x_b}\psi_i\psi_j dx \;,\; F^6=0$$

The order of the variables for the generation of stiffness matrix coefficients are $[u,w,\theta_x,N_{xx},V_x,M_x]$. Both primary and secondary variables are carried as the unknowns in the mixed formulation. The above equations provide the integral forms for the nonlinear system setup for solving the Euler-Bernoulli beam theory. We utilize a C^1 continuous basis function across the knot index space which provides C^1 continuous displacement, and stresses over the domain of interest.

4 FINITE ELEMENT FORMULATION (TBT)

The governing partial differential equations for the variables that enter the finite element formulation for the TBT theory are being (repeated here) for clarity.

$$\frac{\partial N_{xx}}{\partial x}+f_x=0 \;,\quad \frac{\partial M_{xx}}{\partial x}-Q_x=0 \;,\quad \frac{\partial Q_{xx}}{\partial x}+\frac{\partial}{\partial x}\left(N_{xx}\frac{\partial w_0}{\partial x}\right)+q=0$$
$$N_{xx}=EA\left[\frac{\partial u_0}{\partial x}+\frac{1}{2}\left(\frac{\partial w_0}{\partial x}\right)^2\right] \;,\quad M_{xx}=EI\frac{\partial\varphi_x}{\partial x} \;,\quad Q_x=S_{xx}\left[\frac{\partial w_0}{\partial x}+\varphi_x\right] \tag{19}$$

Weak finite element formulation entails the multiplication of the governing partial differential equation with a weight function and integration of the equations over the domain. Following such procedures for the weak form Galerkin finite element formulation the stiffness matrices for the mixed formulation are being presented below (for the Timoshenko beam theory). The order of the variables for the generation of the stiffness matrix coefficients are $[u_i,w_i,\theta_i,N_i,V_i,M_i]$.

$$K^{14}_{ij}=\int_{x_a}^{x_b}\frac{\partial\psi_i}{\partial x}\psi_j dx \;,\; F^1=\int_{x_a}^{x_b}\psi_i f_x dx \;,\; K^{24}_{ij}=\int_{x_a}^{x_b}\left[\frac{\partial\psi_i}{\partial x}\psi_j\frac{\partial\omega_o}{\partial x}\right]dx \;,\; K^{25}_{ij}=\int_{x_a}^{x_b}\left[\frac{\partial\psi_i}{\partial x}\psi_j\right]dx \;,$$
$$F^2=\int_{x_a}^{x_b}\psi_i q_x dx+\left[\psi_i V_{xx}\right]_{x_a}^{x_b} \;,\; K^{35}_{ij}=-\int_{x_a}^{x_b}\psi_i\psi_j dx \;,\; K^{36}_{ij}=\int_{x_a}^{x_b}\psi_i\frac{\partial\psi_j}{\partial x}dx \;,\; F^3=0 \;,$$
$$K^{41}_{ij}=-\int_{x_a}^{x_b}EA\left[\psi_i\frac{\partial\psi_j}{\partial x}\right]dx \;,\; K^{42}_{ij}=-\int_{x_a}^{x_b}\frac{1}{2}EA\psi_i\frac{\partial\psi_j}{\partial x}\left(\frac{\partial\omega_o}{\partial x}\right)dx \;,\; K^{44}_{ij}=\int_{x_a}^{x_b}\psi_i\psi_j dx \;,\; F^4=0 \;, \tag{20}$$
$$K^{52}_{ij}=\int_{x_a}^{x_b}K_sGA\left(\psi_i\frac{\partial\psi_j}{\partial x}\right)dx \;,\; K^{53}_{ij}=\int_{x_a}^{x_b}K_sGA\left[\psi_i\psi_j\right]dx \;,\; K^{55}_{ij}=-\int_{x_a}^{x_b}\psi_i\psi_j dx \;,\; F^5=0 \;,$$

$$K^{63}{}_{ij} = \int_{x_a}^{x_b} EI\left[\psi_i \frac{\partial \psi_j}{\partial x}\right] dx \quad , \quad K^{66}{}_{ij} = -\int_{x_a}^{x_b} \psi_i \psi_j dx \quad , \quad F^6 = 0$$

Both primary and secondary variables are carried as the unknowns in the mixed formulation.

5 B-SPLINE BASIS DEFINITION

One dimensional B-splines are piecewise polynomials. They can be defined as linear combinations of a B-Spline basis. Let us assume we work in the parametric space $\zeta = I$ where *I* is a closed interval of *R*. To define a B-spline basis, the degree of the engendering polynomial *p* and the knot vector need to be specified. Let us denote a knot vector $\zeta = \{\varepsilon_1, \varepsilon_2, \varepsilon_3, \varepsilon_4 ..... \varepsilon_{n+p+1}\}$ as a non-decreasing sequence of real numbers i.e. $\varepsilon_i \le \varepsilon_{i+1}$. In the above sequence of real numbers ε_i are called the knots and ζ the knot vector. The i^{th} b-spline basis function of p-degree (order p+1), denoted by $N_{(i,p)}(\varepsilon)$ is defined below. The zeroth order B-spline functions are defined as:

$$N_{(i,0)} = \begin{cases} 1 & \varepsilon_i \le \varepsilon \prec \varepsilon_{i+1} \\ 0 & otherwise \end{cases} \tag{21}$$

The i^{th} b-spline basis function of p-degree (order $p+1$), denoted by $N_{(i,p)}(\varepsilon)$ is defined as:

$$N_{(i,p)}(\varepsilon) = \frac{\varepsilon - \varepsilon_i}{\varepsilon_{i+p} - \varepsilon_i} N_{i,p-1}(\varepsilon) + \frac{\varepsilon_{i+p+1} - \varepsilon}{\varepsilon_{i+p+1} - \varepsilon_{i+1}} N_{i+1,p-1}(\varepsilon) \tag{22}$$

This is referred to as the Cox-DeBoor recursion formulae. Throughout the paper we assume the knot vector to be open, that is the first and the last knots in the knot vector are interpolator and repeated ($p+1$) times. The basis functions form a partition of unity, besides having other properties of interest as listed below. Partition of unity is expressed as:

$$\sum_{i=1}^{n} N_{(i,p)}(\varepsilon) = 1 \tag{23}$$

The b-spline basis functions possess many desirable properties which enable the use of these functions for solving partial differential equations.

a. $N_{(i,p)}(\varepsilon) = 0$, if ε is outside the interval $\left[\varepsilon_i, \varepsilon_{i+p+1}\right)$.
b. In any given knot span at most $p+1, N_{(i,p)}(\varepsilon)$ are non-zero.
c. Non-negativity of the basis functions. $N_{(i,p)}(\varepsilon) \ge 0$ for all *i* , *p* and ε .
d. Except for the case $p = 0, N_{(i,p)}(\varepsilon)$ attains exactly one maximum value.

6 DERIVATIVES OF B-SPLINE BASIS FUNCTIONS

The derivatives of the b-spline basis are efficiently expressed in a functional form based on b-spline basis of lower order as:

$$\frac{\partial N_{(i,p)}(\varepsilon)}{\partial \varepsilon} = \frac{p}{\varepsilon_{i+p} - \varepsilon_i} N_{i,p-1}(\varepsilon) - \frac{p}{\varepsilon_{i+p+1} - \varepsilon_{i+1}} N_{i+1,p-1}(\varepsilon) \tag{24}$$

Generalizations to higher derivatives is obtained by simply differentiating each side of the above equation to obtain

$$\frac{\partial^k N_{(i,p)}(\varepsilon)}{\partial^k \varepsilon} = \frac{p}{\varepsilon_{i+p} - \varepsilon_i} \frac{\partial^{k-1} N_{(i,p-1)}(\varepsilon)}{\partial^{k-1} \varepsilon} - \frac{p}{\varepsilon_{i+p+1} - \varepsilon_{i+1}} \frac{\partial^{k-1} N_{i+1,p-1}(\varepsilon)_{(i,p)}}{\partial^{k-1} \varepsilon} \tag{25}$$

with the given basis functions we obtain b-spline curves in one dimension. Surfaces in two and three dimensional space are obtained as tensor products of the one-dimensional b-splines. Some affiliated properties of b-spline curves are of further interest in numerical computations and are listed below.

6.1 Affine invariance

Let r be a point in ε^3 (three dimensional Euclidian space). An affine transformation denoted by φ maps ε^3 into ε^3 and has the form

$$\varphi(r) = Ar + v \tag{26}$$

where A is a 3×3 matrix, and v is a vector. Affine transformations include translations, rotations, scaling and shears. Affine invariance property of b-splines follows from the partition of unity property of b-spline basis.

6.2 Strong convex hull

The b-spline curve in one-dimension or surface in two and three dimensions lies in the convex hull of the control points. This property follows from the non-negativity and partition of unity properties of the $N_{ip}(u)$. The tensor product structure in two dimensions requires the b-spline surface in two dimensions to be defined as:

$$S(u,v) = \sum_{i=0}^{n} \sum_{j=0}^{m} N_{(i,p)}(\zeta) N_{(j,p)}(\xi) P_{(i,j)} \tag{27}$$

The tensor product entails the surface formed with a cubic in U and a quadratic b-spline in V. In matrix notation the formation of the tensor product takes the form

$$S(u,v) = \left[N_{(k,p)}(\zeta) \right]^T_{(k,p)} \left[P \right]_{(k,l)} \left[N_{(l,q)}(\zeta) \right]_{(l,q)} \qquad i - p \le k \le i \quad and \quad j - q \le 1 \le j \tag{28}$$

Having examined the b-spline basis functions in detail and described the properties we study the advantages associated with solving beam theories with a NURBS based mixed formulation.

7 BOUNDARY CONDITIONS

The specification of the boundary condition for the beam problem can be achieved based on a number of different ways in which the beam is supported. The different boundary conditions that were examined were the clamped-clamped, pinned-pinned, and hinged-hinged cases. The clamped-clamped case involves specification of the following variables to zero;

$$u = w_0 = \varphi_x = 0 \tag{29}$$

The pinned-pinned case requires the specification of the following variables to be zero;

$$u = w_0 = 0 \tag{30}$$

Also, the specification of the third variable comes from the specification of the end moment, which is zero for the case that the ends are not subject to any external moments. For the mixed formulations, the boundary condition is specified explicitly. Finally, the hinged-hinged case involves the specification of the following variables,

$$w_0 = 0 \tag{31}$$

Since the essential boundary conditions were essentially homogeneous the enforcement of these conditions required no special treatment.

8 LINEARIZATION PROCEDURE

The linearization process can be accomplished with either of two techniques, namely the Picard (direct iteration procedure) or the Newton-Raphson's method. For checking the convergence behavior of both methods of linearization with NURBS both of these were implemented. Some of the advantages of the Newton-Raphson method are a faster convergence rate, since we are using incremental load steps for the runs. The linearized problem with the Newton's method is represented as follows:

$$\left[K^e \left\{ \Delta^e \right\}^r \right]^{\tan} \left\{ \delta\Delta \right\}^e = -\left\{ R^e \right\}^r \tag{32}$$

A direct solver Gauss-Elimination with scaled partial pivoting was used for solving the linear system generated after linearization. The non-linear convergence was declared when the L^2 norm of the incremental vector normalized with the norm of the solution vector was less than 10^{-03} for the FEM models. In the forthcoming sections we present the results that we obtained for the linear and non-linear problems that were studied with different types of boundary conditions.

9 NUMERICAL RESULTS

The TBT beam and the EBT beam were solved with mixed finite element formulation. We present the results with C^1 continuous b-spline basis over the computational domains of interest.

9.1 Linear series solutions

Analytical solutions for the Timoshenko beam theory as also the first order shear deformation theory of plates exist in terms of the Navier solutions in two dimensions. For a complete description of the Navier equations the reader is referred to Reddy [22]. The solution to the problem can be expressed in terms of an infinite series which can be extended to any desired level of accuracy with the help of inclusion of an appropriate number of terms in the infinite expansion. The boundary conditions of simply supported beams are expressed as [22]: $w = 0$ and, $M = 0$, at $x = 0$, L. The linear solution that corresponds to the solution of the Timoshenko Beam Theory are provided. Consider a Timoshenko beam subject to the end deflection of zero and moment to zero. For the case that the beam is subject to a uniform load, expressions for deflections and slopes for the Timoshenko beam elements are;

$$w(x) = \sum_{n=1}^{\infty} \lambda_n \Delta_n \frac{Q_n L^4}{n^4 \pi^4 EI} \sin\left(\frac{n\pi x}{L}\right) \tag{33}$$

$$\varphi(x) = \sum_{n=1}^{\infty} \lambda_n \frac{Q_n L^3}{n^3 \pi^3 EI} \cos(\frac{n\pi x}{L}) \tag{34}$$

where the constants introduced are defined as follows;

$$\lambda_n = \left(1 + n^2 \pi^2 \Omega\right) , \qquad \Omega = \frac{EI}{GAK_s L^2} \tag{35}$$

The linear series solutions provided above serve as a very good estimate to the actual results obtained from the solutions of the NURBS based TBT solutions with mixed formulations. This served as validation benchmarks for the problem solved.

9.2 Nonlinear solutions

The first formulation examined is the NURBS based mixed formulation for EBT, and the second formulation is the NURBS based mixed formulation for TBT. Both of these will be described in the following sections for both beam theories studied.

9.2.1 Euler-Bernoulli beam theory

Results from mixed model are discussed in the following sections when subject to non-linear analysis and different boundary conditions.

Hinged- Hinged B.C. (EBT)

Consider a EBT beam which is subject to hinged-hinged boundary conditions at both ends. The beam length $L = 100in$, $1in \times 1in$ cross section, made of steel ($E = 30msi$), and subjected to a uniform loading of intensity $q_0 1b/in$. The Poisson ratio for the beam was taken as 0.25. The moment of inertia of the beam was taken as 1/12 in^4. For the mixed model the whole domain of the beam was modeled. The geometric boundary conditions for the beam with hinged-hinged boundary condition have been specified earlier. The non-dimensionalization of the deflection was carried out based on equation [37].

A total of 10 elements were used for this analysis, with uniformly spaced knots and uniform p_{level} for the uniform knot considered. The discrete problem resulted in a total of 132 degrees of freedom of the system. A constant p_{value} of 3 was used in each element. A second parametric run was performed based on non-uniform rational basis functions.

The discretization involved a total of 34 b-splines over the computational domain. The number of degrees of freedom for the system were specified as 204 for the NURBS basis. A constant polynomial order of 3 was used in the analysis. A uniform load parameter of 1.0 was used for stepping through the loads till a maximum value of 10 (as reported in Table 1.) was reached. For the mixed formulation each node has a total of six degrees of freedom. As can be seen from Table 1, the agreement with the NURBS based results and the results of Reddy [2] is excellent. The low polynomial order of 3 was used in the problem formulation. Column results with a subscript *N* was used to denote the results obtained for the non-rational basis functions. The maximum percentage error between the mixed model and the reduced integration results of Reddy [2] was found to be 0.05%. Hinged-hinged case is the most sensitive case for verifying the absence of locking issues and it was realized that with appropriate p_{level} refinement there was no need to use reduced integration to obtain excellent results. For the hinged-hinged case the deflection corresponds to the linear case and it is possible to derive w analytically. The maximum deflection at the center of the beam is derived as:

$$w_0(x) = \frac{q_0 L^4}{24EI}\left[\frac{x}{L} - 2\frac{x^3}{L^3} + \frac{x^4}{L^4}\right] \tag{36}$$

From the above expression it follows the maximum deflection is at the mid-span of the beam $x = L/2$ where $w_0(L/2) = 0.5208333$ for $q_0 = 1$. We recover this deflection for the first load case as shown in Table 1.

Table 1
Hinged-Hinged cases results EBT models.

$q(xx)$	Mixed Model (*MX*)			Reddy (04)
	w_0	*w*(dimlss)	w_N	w_0
1	0.52052	1.3013	0.52071	0.5208
2	1.04104	2.6026	1.04142	1.0417
3	1.56156	3.9039	1.56213	1.5625
4	2.08208	5.2052	2.08284	2.0833
5	2.6026	6.5065	2.60355	2.6042
6	3.12312	7.80779	3.12426	3.125
7	3.64364	9.10909	3.64497	3.645
8	4.16416	10.4104	4.16568	4.1667
9	4.68468	11.7117	4.68639	4.6875
10	5.2052	13.013	5.2071	5.2083

Pinned-Pinned B.C. (EBT)

Consider a beam with the material properties defined earlier subject to pinned-pinned boundary conditions. Picard method of linearization was used to obtain the results. The non-dimensional deflections at the center of the beam are also being reported for this beam in Table 2. A total of 10 elements were used for the mixed model. The discrete problem resulted in a total of 132 degrees of freedom of the system. A constant p_{value} of 3 was used in each element. The non-uniform discretization involved a total of 34 b-splines over the computational domain. The number of degrees of freedom for the system were specified as 204 provided for the NURBS basis. A constant polynomial order of 3 was used in the analysis. The uniform load parameter of 1.0 was used for stepping through the loads till a maximum value of 10 (as reported in Table 2.) was reached. In Table 2, subscript *N* has been used to denote the results obtained from the usage of non-uniform rational b-spline basis. For the mixed formulation each node has a total of six degrees of freedom.

Table 2
Pinned-Pinned case results EBT models.

$q(xx)$	Mixed Model (*MX*)			Reddy (04)
	w_0	*w*(dimlss)	w_N	w_0
1	0.368242	0.920606	0.368374	0.3685
2	0.545069	1.36267	0.545257	0.5454
3	0.663559	1.6589	0.663782	0.6640
4	0.755027	1.88757	0.755302	0.7555
5	0.830623	2.07656	0.831012	0.8312
6	0.895685	2.23921	0.896173	0.8964
7	0.954319	2.3858	0.953757	0.9540
8	1.00621	2.51553	1.00559	1.0058
9	1.04868	2.6217	1.05253	1.0531
10	1.09177	2.72943	1.09611	1.0967

Reddy [2] results were obtained with 4 quadratic elements with reduced integration techniques for this case. The maximum percentage error between the two different mixed models was found to be 0.45%. The non-dimensional deflections for the different *a/h* ratios for the pinned-pinned cases were also explored and are presented in Table 3.

Table 3
Pinned-Pinned results for different *a/h* ratios (EBT).

$q(xx)$	Non-dimensional displacements different *a/h* ratios			
	w_{10}	w_{20}	w_{25}	w_{100}
1	1.28097	1.28096	1.28095	0.920606
2	2.58195	2.58193	2.58183	1.36267
3	3.86259	3.86252	3.8622	1.6589
4	5.16324	5.16308	5.1623	1.88757
5	6.42254	6.42224	6.42077	2.07656
6	7.72121	7.72069	7.7181	2.23921
7	9.02235	9.02151	9.01732	2.3858
8	10.3236	10.3224	10.316	2.51553
9	11.5382	11.5364	11.5279	2.6217
10	12.8286	12.8263	12.8144	2.72943

Clamped-Clamped B.C. (EBT)

Consider a beam which is subjected to clamped-clamped boundary conditions at both ends. The beam length was taken as $L = 100in$, $1in \times 1in$ cross section, made of steel ($E = 30msi$), and subject to a uniform loading of intensity $q_0 1lb/in$. The Poisson ratio for the beam was taken as 0.25 and the moment of inertia was taken as 1/12 in^4. Table 4., reports the deflections of the center of the beam subject to the clamped-clamped boundary condition and also the non-dimensional deflections at the center of the beam.

A total of 10 elements were used for this analysis for the mixed model, with uniform elements with a uniform p_{level} in each element. The discrete problem resulted in a total of 132 degrees of freedom of the system. A constant p_{value} of 3 was used in each element. The discretization involved a total of 34 b-splines over the computational domain.

The number of degrees of freedom for the system were specified as 204 provided for the NURBS basis. A constant polynomial order of 3 was used in the analysis. The uniform load parameter of 1.0 was used for stepping through the loads till a maximum value of 10 (as reported in Table 4.) was reached. The discrete problem was solved with Gaussian-Elimination with scaled partial pivoting.

Table 4
Clamped-Clamped case results EBT models.

$q(xx)$	Mixed Model			Reddy [04]
	w_0	w(dimlss)	w_N	w_0
1	0.102524	0.25631	0.103319	0.1035
2	0.200969	0.502422	0.202218	0.2025
3	0.292952	0.732381	0.293808	0.2943
4	0.376644	0.941609	0.377152	0.3777
5	0.451988	1.12997	0.452452	0.4534
6	0.520688	1.30172	0.520465	0.5220
7	0.582825	1.45706	0.58434	0.5845
8	0.64021	1.60052	0.642107	0.6418
9	0.693075	1.73269	0.695669	0.6946
10	0.742087	1.85522	0.74563	0.7436

The results presented above is for the case where $a/h = 100$. The maximum percentage error between the two models was found to be 0.20%. Different *a/h* ratios were analyzed and Table 5. illustrates the non-dimensionalized center deflection as a function of changing length of the beam. For the analysis of the beam deflection with changing lengths of the beam, 10 elements were used, and the full beam was modeled. The p_{level} used was set at a uniform

value of 3 to generate these results. The model consisted of a total of 132 degrees of freedom which was stepped with Picard method.

Table 5
Clamped-Clamped results for different *a/h* ratios (EBT).

$q(xx)$	Non-dimensional displacements different *a/h* ratios			
	w_{10}	w_{20}	w_{25}	w_{100}
1	0.256097	0.256097	0.256097	0.25631
2	0.516195	0.516195	0.516195	0.502422
3	0.772226	0.772226	0.772225	0.732381
4	1.03226	1.03226	1.03226	0.941609
5	1.28402	1.28402	1.28402	1.12997
6	1.54366	1.54366	1.54365	1.30172
7	1.80379	1.80379	1.80378	1.45706
8	2.06395	2.06395	2.06393	1.60052
9	2.30677	2.30676	2.30675	1.73269
10	2.56476	2.56476	2.56473	1.85522

Based on the above observations the non-dimensional load *vs*. deflection curves for clamped-clamped Euler-Bernoulli beams is constant with varying lengths from a range of $a/h = 10$ through a value of $a/h = 75$ and varies significantly only for the case of a slender beam of slenderness ratio $a/h = 100$.

9.2.2 Timoshenko beam theory

Non-linear results obtained with the solutions of the Timoshenko beam theory with the mixed formulation (*MX*) have been outlined with published results in literature.

Hinged-Hinged B.C. (TBT)

Consider a beam which is subjected to hinged-hinged boundary conditions at both ends. The beam length $L = 100in$, $1 \times 1in^2$ cross section, made of steel $E = 30msi$, subject to a uniform loading of intensity $q_0 1b/in$. Moment of inertia of the beam was considered as 0.08333 in^4. The non-dimensionalization of the deflection was carried out based on the following formula;

$$w = \frac{100 * w_{\max} * D_{xx}}{L^4} \tag{37}$$

The non-dimensional deflections at the center of the beam are also being reported for this beam in Table 6. A total of 10 elements were used for this analysis, with constant knot intervals of length 10. The discrete problem resulted in a total of 132 degrees of freedom of the system for the mixed formulation. The discretization involved a total of 34 b-splines over the computational domain for the non-uniform rational b-spline basis functions. The number of degrees of freedom for the system were specified as 204 provided for the NURBS basis. A constant polynomial order of 3 was used in the analysis. The uniform load parameter of 0.50 was used for stepping through the loads till a maximum value of 10 (as reported in Table 6.) was reached. Ten elements were used in the analysis with a p_{value} of 3. As can be seen from Table 6, the agreement with present results and reported results of Reddy [2] is excellent. Table 6 presents the results obtained with mixed formulations when utilizing b-splines with a polynomial expansion of 2. There were 10 elements used for this analysis with the load increment taken as 1.0. The lowest possible (a two point quadrature) was used for performing the numerical integration of the b-splines on the hpk element space. Any lower quadrature requirements will be equivalent to a reduced or a selective integration technique. From the column p-2 NURBS results it is clear there was no locking observed for the problem and the formulation lends itself to a locking free implementation.

Table 6
Hinged-Hinged case results TBT models.

$q(xx)$	Mixed (*MX*)		Reddy (04)		P2 NURBS
	w_0	*w*(dimlss)	w_0	w_N	w_0
1	0.51251	1.28127	0.5208	0.520835	0.519818
2	1.03303	2.58257	1.0417	1.04167	1.03964
3	1.54541	3.86351	1.5625	1.5625	1.55945
4	2.06579	5.16448	2.0833	2.08334	2.07927
5	2.56963	6.42408	2.6042	2.60417	2.59909
6	3.08923	7.72307	3.1250	3.12501	3.11891
7	3.60981	9.02452	3.6458	3.64584	3.63873
8	4.13045	10.3261	4.1667	4.16668	4.15854
9	4.61638	11.541	4.6875	4.68751	4.67836
10	5.13269	12.8317	5.2083	5.20835	5.19818

Pinned-Pinned Boundary Condition (TBT)

Consider a TBT beam with material properties defined earlier subject to pinned-pinned boundary condition. The non-dimensional deflections at the center of the beam are reported for this beam in Table 7. Reddy results were obtained with 4 quadratic elements with reduced integration techniques for this case.

A total of 10 elements were used for this analysis. The discrete problem resulted in a total of 132 degrees of freedom of the system. A constant p_{value} of 3 was used in each element. The uniform load parameter of 1.0 was used for stepping through the loads till a maximum value of 10 (as reported in Table 2.) was reached. As can be seen from Table 7., the agreement of the b-spline mixed results and the results of Reddy [2] is excellent. The non-dimensional deflections for the different $a = h$ ratios for the pinned-pinned cases were also studied and have been presented in Table 8.

Table 7
Pinned-Pinned case results TBT models.

$q(xx)$	Mixed (*MX*)			Reddy (04)
	w_0	*w*(dimlss)	w_N	w_0
1	0.368237	0.920592	0.369262	0.3685
2	0.54502	1.36255	0.54661	0.5454
3	0.663419	1.65855	0.665044	0.6640
4	0.75495	1.88737	0.752304	0.7555
5	0.830631	2.07658	0.828173	0.8312
6	0.895567	2.23892	0.902283	0.8964
7	0.953158	2.38289	0.958572	0.9540
8	1.00499	2.51247	1.01006	1.0058
9	1.05173	2.62932	1.05702	1.0531
10	1.09541	2.73852	1.08737	1.0967

Table 8
Pinned-Pinned results for different *a/h* ratios (TBT).

$Q(xx)$	Non-dimensional displacements different *a/h* ratios			
	w_{10}	w_{20}	w_{25}	w_{100}
1	1.31171	1.28865	1.28587	0.920592
2	2.64392	2.59742	2.59174	1.36255
3	3.9553	3.88569	3.87701	1.65855
4	5.28717	5.19405	5.18208	1.88737
5	6.5767	6.46076	6.44533	2.07658
6	7.90654	7.76699	7.74758	2.23892
7	9.2389	9.07559	9.05171	2.38289
8	10.5714	10.3842	10.3553	2.51247
9	11.8151	11.6056	11.5715	2.62932
10	13.1365	12.9031	12.8628	2.73852

Clamped-Clamped B.C. (TBT)

Consider a beam subjected to clamped-clamped boundary conditions at both ends. The beam length $L = 100in$, $1\times 1in^2$ cross section, made of steel (E=30 msi), and subjected to a uniform loading of intensity $q_0 1b/in$. The Poisson ratio considered was taken as 0.25. Table 9, reports the deflections of the center of the beam subjected to the clamped-clamped boundary condition and also the non-dimensional deflections at the center of the beam obtained with the mixed formulation.

Reddy [2] results were obtained with 4 quadratic elements with reduced integration techniques for this case. A total of 10 elements were used in this analysis, with gradation at the edges of the beam. The discrete problem resulted in a total of 132 degrees of freedom of the system. A constant p_{value} of 3 was used in each element.

Table 9
Clamped-Clamped case results TBT models.

$q(xx)$	Mixed (*MX*)			Reddy [04]
	w_0	*w*(dimlss)	w_N	w_0
1	0.103373	0.258432	0.103441	0.1035
2	0.202281	0.505703	0.202434	0.2025
3	0.293956	0.73489	0.29416	0.2943
4	0.3774	0.943501	0.377701	0.3777
5	0.452944	1.13236	0.453368	0.4534
6	0.52144	1.3036	0.521995	0.5220
7	0.58385	1.45962	0.584529	0.5845
8	0.64106	1.60265	0.641851	0.6418
9	0.693834	1.73459	0.694722	0.6946
10	0.742807	1.85702	0.743778	0.7436

The discretization involved a total of 34 b-splines over the computational domain for the non-uniform rational b-spline basis functions. The number of degrees of freedom for the system were specified as 204 provided for the NURBS basis. A constant polynomial order of 3 was used in the analysis. The uniform load parameter of 0.50 was used for stepping through the loads till a maximum value of 10 was reached. The run presented above is for the case where $a/h = 100$. As can be seen from Table 9., the agreement of the NURBS based mixed results and the results of Reddy [2] is excellent. The maximum error between the mixed model and Reddy [2] results was found to be 0.11%. Different *a/h* ratios analysis were carried out and Table 10., reports the dimensionless center deflection as a function of the changing length of the beam. For the analysis of the beam deflection with changing lengths of the beam, 10 elements were used, and the full beam was modeled. The p_{level} used was set at a uniform value of 3 to

generate the results. As can be seen from the results presented here, an increase in the length of the beam did not cause any deterioration of the results and all the results were obtained with full integration techniques.

Table 10
Clamped-Clamped results for different *a/h* ratios.

$q(xx)$	Non-dimensional displacements different *a/h* ratios			
	w_{10}	w_{20}	w_{25}	w_{100}
1	0.286843	0.263783	0.261016	0.258432
2	0.578167	0.531688	0.52611	0.505703
3	0.864937	0.795403	0.787059	0.73489
4	1.15619	1.06324	1.05209	0.943501
5	1.43818	1.32256	1.30869	1.13236
6	1.72899	1.58999	1.57331	1.3036
7	2.02035	1.85793	1.83843	1.45962
8	2.31174	2.12589	2.10358	1.60265
9	2.58371	2.376	2.35106	1.73459
10	2.87268	2.64173	2.614	1.85702

10 DISCUSSION

Mixed models pose a more difficult problem to solve as compared to displacement based formulations which cause the model to experience significant convergence issues with standard iterative solvers. Direct solvers were found to be able to parse the discrete system. Mixed model however furnish the axial force, shear force, and bending moment as a function of the length along the beam whereas the displacement model can furnish these results only as part of the post processing stage.

Fig. 1 presents the b-spline basis over the computational domain of 100 units of the beam length. For generating the figure the following uniform knot vector was used

$$x = \{0,0,0,0,25,25,50,50,75,75,100,100,100,100\} \tag{38}$$

which provided a total of 14 knots over the domain. The multiplicity of the knots was taken as 2. The number of b-splines for this problem were set to 10 which spanned the domain. For the non-linear problems solved the uniform knot vector for the refined discretization was taken as:

$$x = \{0,0,0,0,10,10,20,20,30,30,40,40,50,50,60,60,70,70,80,80,90,90,100,100,100,100\} \tag{39}$$

with a multiplicity of the knot set to 2. This resulted in ensuring a C^1 basis over the domain. There were 26 knots over the domain with a total of 22 b-splines over the computational domain. A further parametric study was performed with a non-uniform knot vector of

$$x = \begin{Bmatrix} 0,0,0,0,5,5,10,10,17.5,17.5,25,25,31.25,31.25,37.5,37.5,43.75,43.75,50,50,56.25,56.25, \\ 62.5,62.5,68.75,68.75,75,75,82.5,82.5,90,90,95,95,100,100,100,100 \end{Bmatrix} \tag{40}$$

The above specified a non-uniform knot vector with a knot multiplicity of 2. This ensured C^1 continuity across the knot index space. There were a total of 38 knots over the domain with a total of 34 b-splines over the computational domain. Fig. 2 presents the deflection and slope along the length of the beam when analyzed with the NURBS based mixed formulation with the Timoshenko beam theory. A linear analysis was performed. The maximum defection and slopes obtained for the TBT beam was found to be in excellent agreement with spectral/hp results of Ranjan [10] and published analytical solutions of Reddy [22].

Let us consider a total length of the beam as 10 inches described with the TBT. The modulus of elasticity of the beam was taken as 30 *msi*, Area of cross section of the beam was taken as 0.05 in^2. The moment of inertia of the beam was determined to be $1.04167e^{-5}$ in^4. Poisson ratio of the beam was taken as 0.3. We subject the beam to elastic deformation analysis with the Timoshenko beam theory. A linear analysis was performed to verify the convergence history with known analytical solutions available for the problem in the form of series expansions.

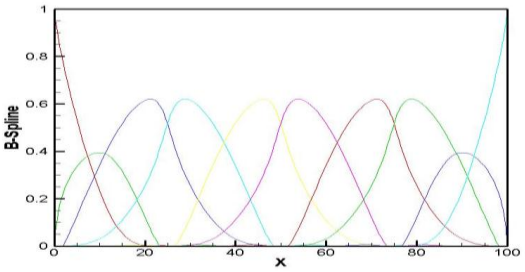

Fig.1
B-splines over the computational domain for given knot vector.

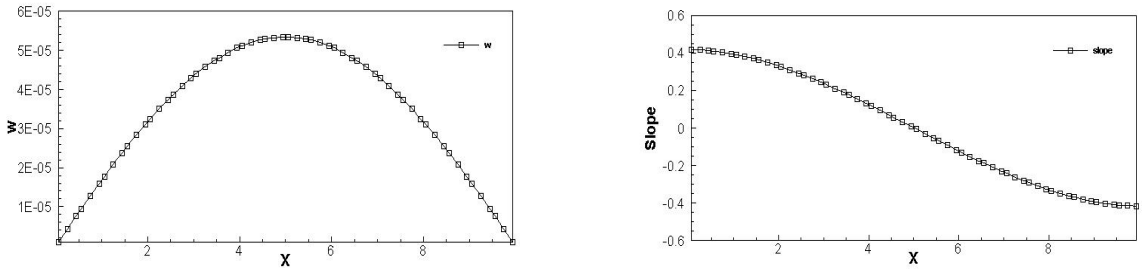

Fig.2
Deflection and slope series solutions TBT theory.

Fig. 3 presents the L^2 convergence of the deflections and slopes with non-uniform rational b-spline basis with increasing polynomial orders along with previously published spectral/hp convergence results from Ranjan [13]. Discrete values of polynomial orders of the NURBS basis of (2, 3, 4, 5, and 7) were examined to study the convergence history. A conforming C^1 continuous NURBS vector space was determined to describe the solution for the problem. As an example the knot vector for the polynomial order of 5 was taken as:

$$x = \{0,0,0,0,0,0,2.5,2.5,2.5,2.5,5,5,5,5,5,7,5,7.5,7.5,7.5,10,10,10,10,10,10\} \tag{41}$$

We observe exponential convergence history of both the deflections and slopes for the problem on a semi log plot with increasing polynomial order. The NUBBS basis provides superior convergence than the spectral/hp results of Ranjan [13] and attains machine accuracy by the expansion order 4. This is attributed to an appropriate k-continuous expansion which respects C^1 continuity of each of the variables in the problem.

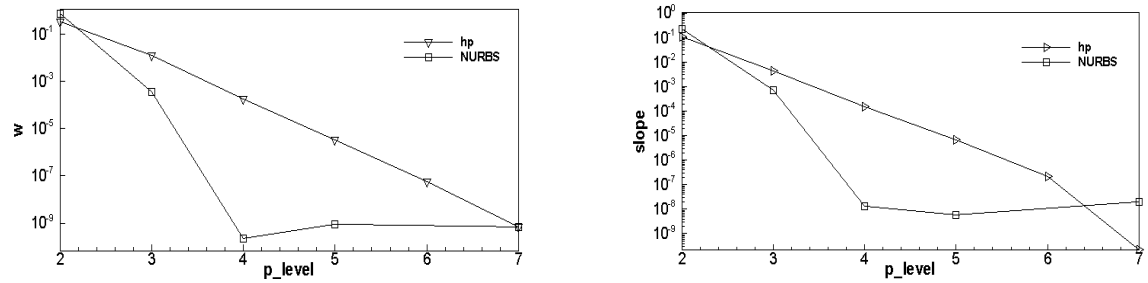

Fig.3
Convergence of deflection and slopes for NURBS and spectral/hp results.

Fig. 4 presents the shear and moment along the length of an EBT beam subject to pinned-pinned boundary conditions at the end of the first load step. The shear and moment obtained along the length of the beam with NURBS based mixed formulation and spectral/hp methods are being provided. The usage of NURBS with a higher continuity across the knot index space clearly recovers the constant state of shear along the beam length where as an hp framework provided by the spectral/hp methods recovers irregular shear along the length. The moments obtained with the earlier spectral/hp results of Ranjan [10] and the present results were found to be excellent. Fig. 5 presents mixed formulation results for the load versus deflection curves with different slenderness ratios for a EBT beam subject to pinned-pinned boundary conditions. Fig. 6 presents load vs. deflection curves for the EBT model with clamped-clamped boundary conditions for different slenderness ratios. In Fig. 7 we present load versus deflection curves for the pinned-pinned TBT beam as a function of different slenderness ratios. A corresponding load versus deflection behavior for the clamped-clamped beam has been presented in Fig. 8 for different slenderness ratios.

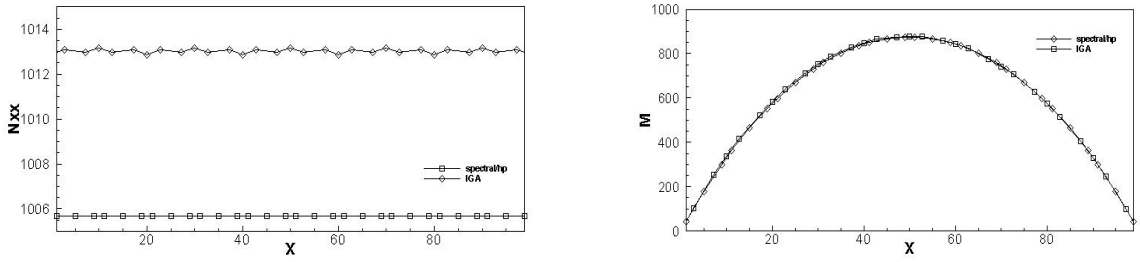

Fig.4
Axial force (*Nxx*) and moment (*V*) for spectral/hp and NURBS results.

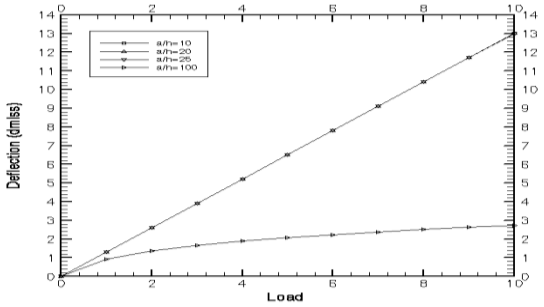

Fig.5
Non-dimensional deflection *vs*. load for pinned-pinned boundary condition for different slenderness ratio for EBT.

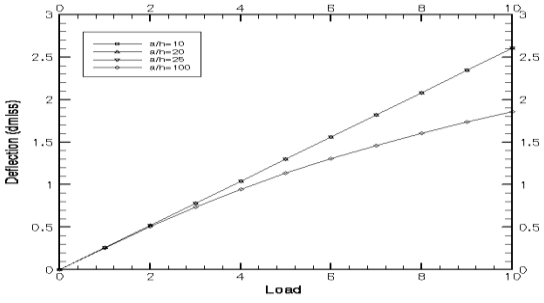

Fig.6
Non-dimensional deflection *vs*. load for clamped-clamped condition for different slenderness ratios for EBT beam.

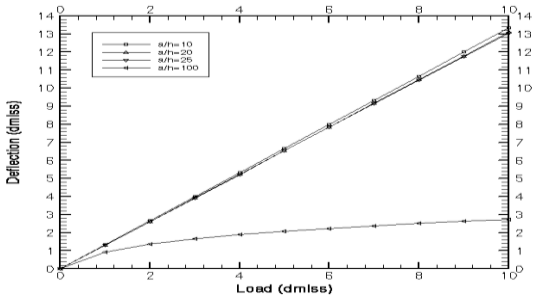

Fig.7
Load *vs*. non-dimensional deflection curves for Pinned-Pinned TBT beam for different slenderness ratios.

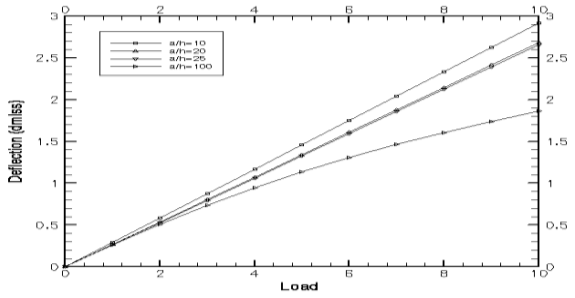

Fig.8
Load vs. non-dimensional deflection curves for CC TBT beam for different slenderness ratios.

11 CONCLUSIONS

Through this work we have demonstrated the usage of b-spline mixed finite element method as a viable tool for predicting the bending response of both Euler-Bernoulli beam and Timoshenko beam models with mixed formulations. We also advocate the usage of b-spline basis for predicting the bending response of beams with mixed formulations to obtain reliable results with full-integration techniques both for linear and non-linear problems. Direct evaluation of secondary variables of the displacement formulations from the mixed formulation is one of the primary advantages offered by the mixed formulation. The usage of b-spline mixed finite element formulation also alleviates perennial problems of ill-conditioning of the stiffness matrices obtained with the usage of higher-order equi-spaced Lagrange basis and provides an adjustable continuity which is very useful for even solving problems in the strong form of the partial differential equations (collocation based approaches).

REFERENCES

[1] Reddy J.N., Wang C., Lee K., 1997, Relationships between bending solutions of classical and shear deformation beam theories, *International Journal of Solids and Structures* **34**(26): 3373-3384.

[2] Reddy J.N., 2014, *An Introduction to Nonlinear Finite Element Analysis: with Applications to Heat Transfer Fluid Mechanics, and Solid Mechanics,* OUP Oxford.

[3] Reddy J.N., Wang C., Lam K., 1997, Unified finite elements based on the classical and shear deformation theories of beams and axisymmetric circular plates, *Communications in Numerical Methods in Engineering* **13**(6): 495-510.

[4] Severn R., 1970, Inclusion of shear deflection in the stiffness matrix for a beam element, *The Journal of Strain Analysis for Engineering Design* **5**(4): 239-241.

[5] Reddy J.N., 1997, On locking-free shear deformable beam finite elements, *Computer Methods in Applied Mechanics and Engineering* **149**(1): 113-132.

[6] Oden J.T., Reddy J.N., 2012, *Variational Methods in Theoretical Mechanics*, Springer Science & Business Media.

[7] Arciniega R., Reddy J.N., 2007, Large deformation analysis of functionally graded shells, *International Journal of Solids and Structures* **44**(6): 2036-2052.

[8] Karniadakis G., Sherwin S., 2013, *Spectral/hp Element Methods for Computational Fluid Dynamics*, Oxford University Press.

[9] Melenk J.M., 2002, On condition numbers in hp-fem with gauss-Lobatto-based shape functions, *Journal of Computational and Applied Mathematics* **139**(1): 21-48.

[10] Ranjan R., Feng Y., Chronopolous A., 2016, Augmented stabilized and Galerkin least squares formulations, *Journal of Mathematics Research* **8** (6): 1-12.

[11] Ranjan R., Chronopolous A., Feng Y., 2016, Computational algorithms for solving spectral/hp stabilized incompressible flow problems, *Journal of Mathematics Research* **8**(4): 1-19.

[12] Ranjan R., Reddy J.N., 2009, Hp-spectral finite element analysis of shear deformable beams and plates, *Journal of Solid Mechanics* **1**(3): 245-259.

[13] Ranjan R., 2011, Nonlinear finite element analysis of bending of straight beams using hp-spectral approximations, *Journal of Solid Mechanics* **3**(1): 96-113.

[14] Da Veiga L.B., Lovadina C., Reali A., 2012, Avoiding shear locking for the timoshenko beam problem via isogeometric collocation methods, *Computer Methods in Applied Mechanics and Engineering* **241**: 38-51.

[15] Tran L.V., Ferreira A., Nguyen-Xuan H., 2013, Isogeometric analysis of functionally graded plates using higher-order shear deformation theory, *Composites Part B*: *Engineering* **51**: 368-383.

[16] Ranjan R., 2010, *Hp-spectral Methods for Structural Mechanics and Fluid Dynamics Problems,* Texas A&M University, Ph.D. Thesis.

[17] Cottrell J.A., Hughes T.J., Bazilevs Y., 2009, *Isogeometric Analysis: Toward Integration of CAD and FEA,* John Wiley & Sons.
[18] Reali A., Gomez H., 2015, An isogeometric collocation approach for Bernoulli Euler beams and Kirchhoff plates, *Computer Methods in Applied Mechanics and Engineering* **284**: 623-636.
[19] Weeger O., Wever U., Simeon B., 2013, Isogeometric analysis of nonlinear Euler-Bernoulli beam vibrations, *Nonlinear Dynamics* **72**(4): 813-835.
[20] Thai C.H., Nguyen-Xuan H., Bordas S., Nguyen-Thanh N., Rabczuk T., 2015, Isogeometric analysis of laminated composite plates using the higher-order shear deformation theory, *Mechanics of Advanced Materials and Structures* **22**(6): 451-469.
[21] Kapoor H., Kapania R., 2012, Geometrically nonlinear nurbs isogeometric finite element analysis of laminated composite plates, *Composite Structures* **94**(12): 3434-3447.
[22] Reddy J.N., 2006, *Theory and Analysis of Elastic Plates and Shells*, CRC press.